

## Dimensionality-dependent energy transfer in polymer-intercalated SnS<sub>2</sub> nanocomposites

P. Parkinson,<sup>1,\*</sup> E. Aharon,<sup>2</sup> M. H. Chang,<sup>1</sup> C. Dosche,<sup>3</sup> G. L. Frey,<sup>2</sup> A. Köhler,<sup>3</sup> and L. M. Herz<sup>1,†</sup>

<sup>1</sup>Clarendon Laboratory, Parks Road, Oxford OX1 3PU, United Kingdom

<sup>2</sup>Department of Materials Engineering, Technion-Israel Institute of Technology, Haifa 32000, Israel

<sup>3</sup>Institute of Physics, University of Potsdam, Am Neuen Palais, Potsdam 14469, Germany

(Received 14 December 2006; published 30 April 2007)

We have investigated the influence of dimensionality on the excitation-transfer dynamics in a conjugated polymer blend. Using time-resolved photoluminescence spectroscopy, we have measured the transfer transients for both a three-dimensional blend film and for quasi-two-dimensional monolayers formed through intercalation of the polymer blend between the crystal planes of an inorganic SnS<sub>2</sub> matrix. We compare the experimental data with a simple, dimensionality-dependent model based on electronic coupling between electronic transition moments taken to be point dipoles. Within this approximation, the energy-transfer dynamics is found to adopt a three-dimensional character in the solid film and a two-dimensional nature in the monolayers present in the SnS<sub>2</sub>-polymer nanocomposite.

DOI: 10.1103/PhysRevB.75.165206

PACS number(s): 78.30.Jw, 78.47.+p, 78.66.Qn, 78.55.-m

### I. INTRODUCTION

Conjugated molecular materials have enjoyed 40 years of intensive research, since the discovery of electroluminescence in anthracene in 1962.<sup>1</sup> More recently, advances in chemical synthesis have led to the development of conjugated polymers for optoelectronic applications ranging from highly sensitive chemical sensors<sup>2</sup> to solar cells<sup>3</sup> and high-efficiency organic light-emitting diodes.<sup>4</sup> However, optimization of the underlying mechanism behind these applications requires knowledge of the excitation dynamics both along and between the polymer strands in these molecular materials. Many physical aspects of polymer systems affect their optoelectronic properties. In particular, the chain arrangement in the solid<sup>5,6</sup> and the associated electronic coupling between the chains<sup>7</sup> are known to alter profoundly the charge transfer and excitation dynamics in these materials. The dimensionality of these systems plays an important role here, with one-dimensional transfer of excitations along the chain typically being much slower than that within a three-dimensional polymeric solid.<sup>8-11</sup>

One of the advantages of organic semiconductors over inorganics is the wide tunability of the band gap through simple changes in the chemical structure. This has led to a rapid expansion in the applications of full-color light-emitting displays incorporating organic materials and fueled work towards stable white-light-emitting diodes.<sup>12</sup> One promising approach has been the blending of various conjugated polymers, each with a different emission wavelength.<sup>13,14</sup> A disadvantage of this method is that ultrafast energy transfer from the high-energy to the low-energy band-gap component of the blend rapidly quenches the photoluminescence from the blue end of the spectrum. This strong interaction between the components makes such materials extremely sensitive to doping levels and film morphology, both of which may in turn be influenced by processing conditions and change over time. An alternative approach suggested by Aharon *et al.*<sup>15,16</sup> is based on the confinement of the polymer blend in the interlayer galleries of an inorganic semiconducting material that is largely transparent

over the visible spectrum. The formation of quasi-two-dimensional polymer monolayers within this nanocomposite should inhibit energy transfer between the polymer blend components, allowing stable tuning of the apparent emission color though changes in the blend composition. Using this approach, stable white-light emission has recently been demonstrated for a nanocomposite containing a blend of three polymers emitting in the blue, green, and red part of the visible spectrum.<sup>15</sup> The inorganic interlayers may have the additional functions of aiding charge carrier injection<sup>15</sup> and protecting the polymer against degradation through encapsulation.

In this paper, we present a study of how the energy transfer dynamics in a conjugated polymer solid are altered when moving from a three-dimensional (3D) film to a quasi-2D monolayer created by polymer intercalation into SnS<sub>2</sub>. Through measuring the decay of the blue-light-emitting polymer component (the “donor”) in both the presence and absence of green- and red-light-emitting polymers (the “acceptor”) we assess experimentally the excitation transfer rate from the donor to the acceptor. Comparison of our data with a simple model that extends Förster’s theory<sup>17</sup> for resonant dipole-dipole electronic coupling to systems of different dimensionality indicates that polymer intercalation into an inorganic matrix indeed results in excitation transfer characteristic of a truly two-dimensional polymeric solid.

### II. EXPERIMENT

Polymer blend monolayer (2D) samples were fabricated by intercalation of polymer material into SnS<sub>2</sub> as described in Ref. 15. This procedure is based on the exfoliation-adsorption technique, in which an inorganic host material (SnS<sub>2</sub> in our case) is delaminated in solution into single sheets that then restack in the presence of the conjugated polymer. After polymer incorporation, the mixture was repeatedly washed in organic solvents to remove excess polymer not enclosed in the inorganic matrix. The resulting material was redispersed in xylene and deposited on silica substrates through drop casting. X-ray diffraction measurements on

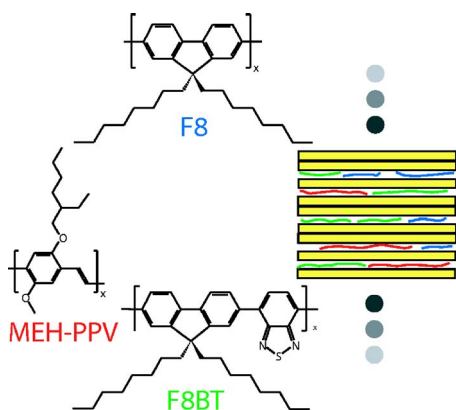


FIG. 1. (Color online) Chemical structures of the three conjugated polymers used for this study. The schematic diagram illustrates the type of layered composite formed when the polymer blend is intercalated between layers of inorganic SnS<sub>2</sub> crystal.

these nanocomposites showed a peak corresponding to the 0.58-nm *c*-axis spacing of SnS<sub>2</sub> crystals and an additional peak at 1.04 nm corresponding to a crystal interlayer expansion of 0.46 nm through incorporation of the polymer.<sup>15</sup> This expansion is of similar magnitude to that reported for related polymer-intercalated materials.<sup>18</sup> It is caused by the tendency of conjugated polymers to adopt a planar conformation in layered compounds,<sup>15</sup> indicating that a single monolayer of polymer forms between SnS<sub>2</sub> layers. Two types of nanocomposites were prepared: one incorporated a blend of blue-light-emitting F8, green-light-emitting F8BT, and red-light-emitting MEH-PPV at a weight ratio of 30:60:10, respectively. A reference composite incorporated only F8 to allow the examination of the donor luminescence in the absence of the acceptors and another composite incorporated only MEH-PPV to allow the examination of the acceptor luminescence in the absence of the donor. Figure 1 shows the chemical structures of all polymers used and schematically depicts a polymer-intercalated SnS<sub>2</sub> crystal. In addition, 100-nm-thick (3D) polymer films were prepared by spin-casting either the F8:F8BT:MEH-PPV blend or just F8 from solution in xylene onto silica substrates. The molecular weights of the polymers used were 74 000 and 16 000 for F8 and F8BT (both purchased from American Dye Source) and 50 000 for MEH-PPV (purchased from Aldrich).

To investigate the energy-transfer dynamics in these materials, time-resolved photoluminescence (PL) up-conversion (UC) was used.<sup>19</sup> The sample was excited by frequency-doubling the output from a mode-locked Ti:sapphire laser (Spectra-Physics Tsunami) supplying 80-fs pulses at a 80-MHz repetition rate. The excitation energy was set to either 2.88 eV to excite MEH-PPV or 3.1 eV to excite F8 preferentially. The excitation beam was focused onto a spot size of 200 μm at powers below 1 mW adjusted to ensure that no sample degradation occurred during the measurement. All experiments were carried out with the sample held under vacuum (<10<sup>-4</sup> mbar) and were fully reproducible. The photoluminescence was collected using a pair of off-axis parabolic mirrors and focused onto a β-barium-borate (BBO) crystal to overlap with a gate pulse at the laser fundamental arriving with a variable time delay. The emerging sum-

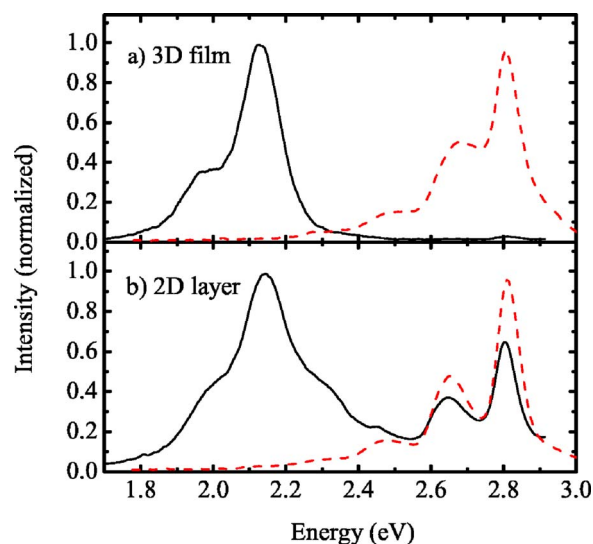


FIG. 2. (Color online) Time-integrated photoluminescence spectra for pristine F8 (dashed line, red) and for the F8:F8BT:MEH-PPV blend (solid line, black) for the case of (a) thin-film (3D) samples and (b) SnS<sub>2</sub> nanocomposites intercalated with 2D polymer monolayers.

frequency photons were then coupled into a spectrometer and detected using a liquid-nitrogen-cooled charge-coupled device (CCD). The temporal resolution of the system was approximately 300 fs as determined from the measured width of the excitation pulse. In this geometry the system detects the photoluminescence with polarization parallel to the gate beam and the excitation beam was chosen to have a polarization parallel to this. The time-integrated PL spectra were measured using an Edinburgh instruments FLS920 spectrometer.

### III. RESULTS

Figure 2 shows the time-integrated photoluminescence spectra of F8 and the blend for (a) the 3D thin film and (b) the 2D monolayers included in the nanocomposites. For all spectra shown, the samples were excited at an energy of 3.1 eV, creating excitons mainly on the F8 donor. The F8 thin film and the corresponding nanocomposite show an emission peak at 2.82 eV and a progression at 2.67 eV, mediated by C-C stretch vibrations. However, with addition of the F8BT:MEH-PPV acceptor the thin-film luminescence becomes dominated by MEH-PPV, whose vibronic emission peaks may be observed at 2.15 eV, 1.96 eV, and 1.8 eV. The almost complete quenching of both F8 and F8BT luminescence in the blend film indicates an efficient energy transfer to the polymer with the lowest band gap. The nanocomposite incorporating the blend, on the other hand, shows contributions to the emission from all three polymers, suggesting that the energy-transfer efficiency in the 2D layers of the nanocomposites is significantly reduced. As a result, the emission from the nanocomposite seems white to the eye, in contrast to the red appearance of the emission from the thin film. In order to obtain information about the rate (and therefore mechanism) of exciton migration from donor to acceptor,

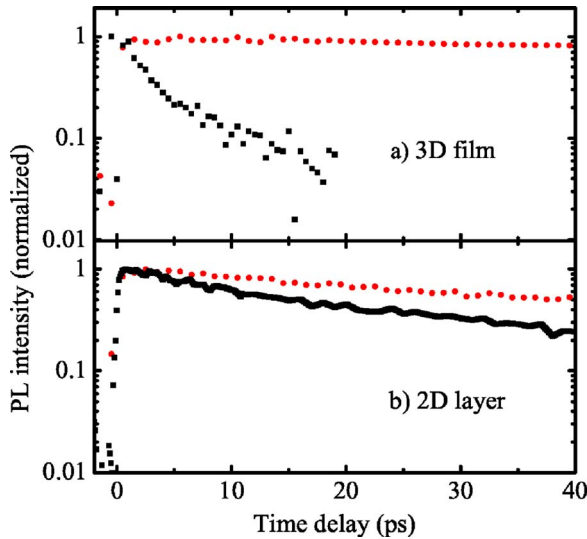


FIG. 3. (Color online) Time-resolved photoluminescence decay measured at 2.67 eV. Both the PL from pristine F8 (circles, red) and the PL from F8 in the polymer blend (squares, black) are shown for (a) a 3D thin film and (b) 2D layers incorporated into a  $\text{SnS}_2$  nanocomposite. The decay of the F8 emission can be seen to accelerate slightly upon intercalation as F8 also couples weakly to the  $\text{SnS}_2$  matrix, which features an absorption onset in the UV region (Ref. 15).

time-resolved photoluminescence measurements were carried out to determine the exciton population on F8 and MEH-PPV. Figure 3 shows the decay of the F8 (donor) emission (at 2.67 eV) for pristine F8 and for F8:F8BT:MEH-PPV blends, for both a thin-film (a) and a  $\text{SnS}_2$  nanocomposite (b) sample. The decay of the PL from the F8 donor in both the thin film and the nanocomposite becomes more rapid with the addition of the F8BT:MEH-PPV acceptor, confirming that energy transfer occurs from donor to acceptor. The relative change in this decay rate is considerably more rapid in

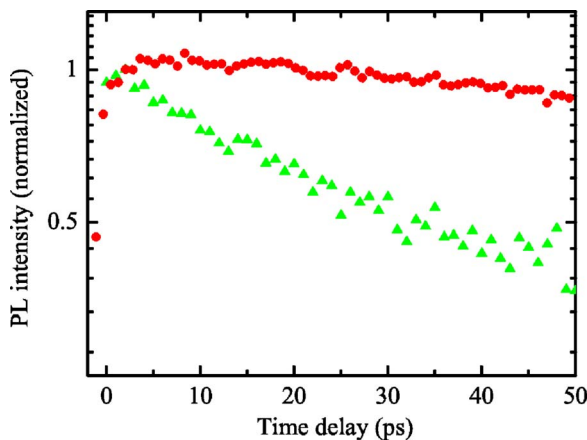


FIG. 4. (Color online) Time-resolved photoluminescence decay measured at 2.16 eV. Both the PL from pristine MEH-PPV intercalated into the  $\text{SnS}_2$  nanocomposite (triangles, green) and the PL from MEH-PPV in the polymer blend in the  $\text{SnS}_2$  nanocomposite (circles, red) are shown. An excitation energy of 3.1 eV was used for the polymer-blend  $\text{SnS}_2$ , while an excitation energy of 2.8 eV was used for the pristine MEH-PPV- $\text{SnS}_2$  composite.

the thin-film samples than the nanocomposite, suggesting that the nature of the transfer mechanism is strongly modified when moving from a 3D film to a 2D monolayer. For comparison, Fig. 4 displays the time-resolved photoluminescence from MEH-PPV (at 2.16 eV) both for pristine MEH-PPV intercalated in  $\text{SnS}_2$  and for the F8:F8BT:MEH-PPV blend intercalated in  $\text{SnS}_2$ . The pristine MEH-PPV incorporated in  $\text{SnS}_2$  nanocomposite was directly excited at 2.81 eV, and the PL decay is representative of the exciton lifetime on MEH-PPV in the composite. For the F8:F8BT:MEH-PPV blend intercalated in  $\text{SnS}_2$ , excitation at 3.1 eV predominantly created excitons on F8. Here, a delayed rise in the MEH-PPV emission can be observed with an increase in the apparent PL lifetime, in accordance with energy transfer from the donor. However, the dynamics of the MEH-PPV emission in the blend is complex, with the exciton density on the polymer being fed not only by excitation transfer from F8 and F8BT, but also through direct excitation by the laser pulse, which is difficult to quantify accurately. For the remainder of this study we will therefore focus on the analysis of the donor emission from the materials.

#### IV. DISCUSSION

Theoretical discussion of energy transfer in  $\pi$ -conjugated donor-acceptor systems generally relies on electric-dipole coupling between the emitting transition moment of the donor and the absorptive transition moment of the acceptor.<sup>20</sup> The simplest approximation here is based on interactions between point dipoles and has been repeatedly applied to conjugated polymeric systems.<sup>21–25</sup> For this case, the rate of transfer  $k$  was calculated by Förster<sup>17</sup> to be inversely proportional to the sixth power of the acceptor-donor separation  $r$ ,

$$k(r) = \frac{1}{\tau} \left( \frac{R_0}{r} \right)^6, \quad (1)$$

where  $\tau$  is the excitation lifetime for the donor in the absence of the acceptor and  $R_0$  is the Förster radius characteristic for the system. However, for an ensemble of randomly distributed chromophores, a range of acceptor-donor distances will be present in the material, requiring an ensemble average to be determined that will also depend on the dimensionality of the system. To analyze the temporal evolution of the excitation within this approximation, we follow the procedure outlined by Baumann and Fayer<sup>23</sup> and apply it to the case of a single type of donor. First, we consider only the deexcitation path for the donor that results from energy transfer and define the probability of an excitation remaining on the donor molecule as

$$E(t, r) = e^{-k(r)t}. \quad (2)$$

We can rule out retransfer of excitation from acceptor to donor chromophore as a result of the negligible spectral overlap of donor absorption with acceptor photoluminescence for our materials. In addition, the relatively small overlap between the donor absorption and its own emission that is typical of conjugated materials with torsional degrees of freedom<sup>26,27</sup> allows us to neglect exciton migration within

the donor at the high acceptor concentration employed here. This permits the simplification of the full treatment by Baumann and Fayer<sup>23</sup> and Blumen and Manz<sup>28</sup> as outlined in the following. Assuming a random ordering of donors and acceptors, the configurational average of the probability of finding an initially excited donor still excited at time  $t$  is

$$G(t) = \prod_{i=1}^N (1-p) + pE(t, r_i), \quad (3)$$

where  $p$  is the probability that a site contains an acceptor and the product extends over  $N$  molecular sites. By expanding the logarithm of Eq. (3), we obtain

$$\ln G(t) = - \sum_{h=1}^{\infty} \frac{p^h}{h} \sum_{i=1}^N [1 - E(t, r_i)]^h. \quad (4)$$

The summation over individual sites may then be replaced by an integration over all space, if a continuous spatial distribution is assumed:

$$\ln G(t) = - \rho \phi(p, \Delta) \int_0^{\infty} (1 - e^{-k(r)t}) u(r) dr. \quad (5)$$

Here,  $\rho$  is a number density of acceptors,  $\phi(p, \Delta)$  is a scaling factor related to the proportion of acceptors  $p$  and the number of spatial dimensions of the material  $\Delta$ , and  $u(r)dr$  is the probability of finding an acceptor molecule within the distance  $[r, r+dr]$  from the donor, multiplied by the dimension-specific volume element. At this point, the effect of dimensionality of the system enters, with the two-dimensional and three-dimensional random acceptor distributions given through  $u_{2d}(r) = 2\pi r$  and  $u_{3d}(r) = 4\pi r^2$ , respectively. By using as substitutions

$$\mu = \frac{t}{\tau} R_0^6 \quad \text{and} \quad y = \frac{\mu}{r^6}, \quad (6)$$

$G(t)$  may be simplified for the two- and three-dimensional cases as

$$\ln G_{2D}(t) = - 2\pi\rho\phi(p, \Delta)\mu^{1/3} \int_0^{\infty} (1 - e^{-y})y^{-4/3} dy, \quad (7)$$

$$\ln G_{3D}(t) = - 4\pi\rho\phi(p, \Delta)\mu^{1/2} \int_0^{\infty} (1 - e^{-y})y^{-3/2} dy. \quad (8)$$

The integral is independent of  $t$  and reduces to a  $\gamma$  function.<sup>29</sup> The time dependence of the excitation transfer from the donor,  $G(t)$ , is solely determined by  $\mu$ , which in turn is influenced by the number of spatial dimensions. We may therefore express the expected time-dependent PL decay of the donor as a result of energy transfer as

$$G(t) = G_0 e^{-(t/t_0)^\alpha}, \quad (9)$$

where the  $t_0$  is a system-specific time constant related to  $R_0$ ,  $\phi$ , the acceptor concentration, and the donor's excited-state lifetime. The dependence of  $t_0$  on  $\phi$  and therefore the dimensionality complicates the analysis and prohibits a meaningful value of  $R_0$  from being obtained. The exponent  $\alpha$  depends on

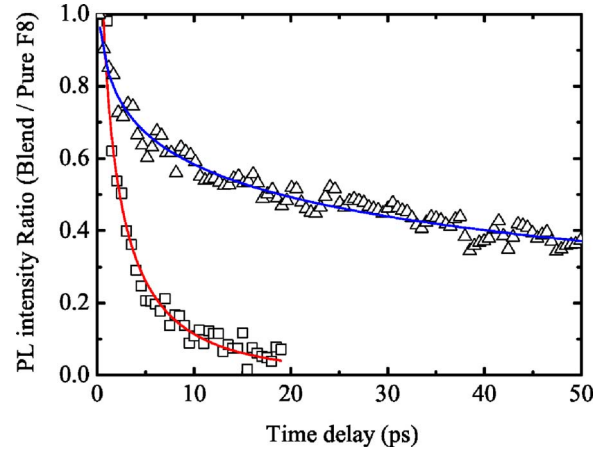


FIG. 5. (Color online) Excitation-transfer transients, defined as the ratio between the photoluminescence intensity of F8 without acceptor and that with acceptor, shown for both a 3D solid film (squares) and 2D monolayers incorporated in SnS<sub>2</sub> composites (triangles). The solid lines are numerical fits to the data using the model described in the text.

the number of dimensions in which energy transfer can occur through  $\alpha = \Delta/6$ , so  $\alpha = 1/3$  and  $\alpha = 1/2$  should be expected for a two-dimensional and a three-dimensional system, respectively.

The experimental data displayed in Fig. 3 are influenced by deexcitation of the donor through all available mechanisms, while Eq. (9) is based on energy transfer as the only pathway. To extract information on just the energy-transfer rate from the data, we consider that the decay of exciton population  $f$  in the materials containing only the donor polymer may be described by the following rate equation:

$$\frac{d}{dt}f = - \left( \frac{1}{\tau} + r(t) \right) f(t), \quad (10)$$

where  $\tau$  is the natural exciton lifetime and  $r(t)$  is a time-dependent decay rate associated with processes such as exciton diffusion to nonradiative traps. In the presence of the F8BT:MEH-PPV acceptor, the exciton population on the F8 donor  $g$  experiences additional losses,

$$\frac{d}{dt}g = - \left( \frac{1}{\tau} + r(t) \right) g(t) - K(t)g(t), \quad (11)$$

where  $K(t)$  represents the time-dependent energy-transfer rate from donor to acceptor ensemble. It can be shown<sup>25</sup> that within the point-dipole model described above, the ratio  $I(t) = f(t)/g(t)$  is directly related to  $K(t)$  and follows the time dependence of  $G(t)$  given in Eq. (9).

Figure 5 displays the experimental data for  $I(t)$  obtained by division of the F8 emission from the blend by that from the materials containing F8 as the only polymer, for both the case of the 3D polymer film and the 2D monolayer. Superimposed on the data are the best fits based on stretched exponentials<sup>30</sup> as given by Eq. (9) with  $\alpha$ ,  $G_0$ , and  $t_0$  as free parameters. For monolayers enclosed in the SnS<sub>2</sub> nanocomposites we obtain  $\alpha = 0.31 \pm 0.04$ , while the thin film yields  $\alpha = 0.47 \pm 0.07$ , close to the values of 0.33 and 0.5 to be ex-

pected for the case of two-dimensional and three-dimensional transfer, respectively.

The excellent agreement between this simple model and the experimental data seems surprising at first, given the complexity of the system. First, one might raise the question of whether electronic coupling *between* adjacent polymer monolayers in the nanocomposites also has to be considered. X-ray diffraction from the composites<sup>15</sup> points to the existence of extended SnS<sub>2</sub> crystalline domains, indicating that only a fraction of the adjacent crystal sheets incorporate polymer upon restacking in solution. As a result, the polymer monolayers are sufficiently isolated in the crystal to be considered as noninteracting two-dimensional systems. Another possible complication is that phase segregation between the components of the polymer blend might lead to a nonrandom local distribution in both the solid film and the nanocomposites. However, photoluminescence microscopy experiments with 200-nm resolution have indicated uniform distribution of all components.<sup>15</sup> In addition, no residual donor luminescence is observed at long times after excitation or in the time-integrated spectra, pointing towards a complete transfer of excitation and therefore the absence of large homogeneous donor domains. The two indicators taken together suggest that phase segregation, if present, may only exist over distances that are comparable with the energy-transfer range. While the analysis presented above is strictly valid for a two-component system and this sample has three, the effect of having two acceptors for the F8 donor to transfer energy only alters the effective lifetime  $t_0$  in Eq. (9) and thus has no effect on the extracted dimensionality.

Finally, the validity of the point-dipole approximation used in our derivation needs to be examined with care. Quantum chemical calculations predict that an initially created exciton on a conjugated polymer chain is delocalized over a few repeat units.<sup>8,9</sup> Subsequent lattice relaxation over a typical nuclear vibration period will lead to a localization of the exciton with a resulting wave function extent of the order of 1 nm. Energy transfer over similar length scales is then expected to deviate from calculations using the simple point-dipole approximation. To overcome these limitations, alternative models have been based on line-dipole<sup>31</sup> or distributed monopole<sup>8,9</sup> approaches. The latter predicts an increase of the transfer rate between two conjugated oligomers in head-to-tail geometry and a decrease for a cofacial arrangement in comparison with the simpler point-dipole approximation. The two counteracting effects make it hard to assess qualitatively the overall effect on a solid comprising an ensemble of conjugated oligomers, while a quantitative picture would re-

quire demanding computational simulations on generated random morphologies that take proper account of the physical space occupied by the donor and acceptor molecules. For the systems investigated here, deviations from the point-dipole approximation are most likely to be observed for the 3D solid films, for which chains may pack cofacially at distances as short as 3–8 Å.<sup>32</sup> For the SnS<sub>2</sub> nanocomposites the arrangement of a 2D polymer monolayer inhibits such cofacial arrangements, leading to a significant increase in the smallest distances over which excitation transfer may occur. As a result, the point-dipole approximation is expected to hold for the case of a 2D polymer monolayer incorporated in this type of nanocomposite.

## V. CONCLUSION

We have examined the dependence of dimensionality on the energy transfer in conjugated polymer blends. For the three-dimensional blend film, excitation transfer from the donor is almost completed within the first few picoseconds. Intercalation of quasi-two-dimensional polymer monolayers into an inorganic matrix results in slower excitation transfer, which occurs over the time scale of a few tens of picoseconds. For both systems, the transfer dynamics can be described by a stretched exponential with a dimensionality-dependent exponent. A simple model was outlined that is based on excitation transfer through electronic coupling between transition moments considered to be point dipoles and takes account of the system dimensionality. Comparison with the experimental data indicates that within these approximations, energy transfer occurs in three dimensions for the solid film, but only in two dimensions when the polymer is incorporated as a monolayer in the SnS<sub>2</sub> nanocomposites. The resulting decrease of the overall rate at which energy is transferred to the lowest-energy component means that emission is clearly observed from all components of the polymer blend incorporated in the nanocomposites. Achieving this task through a reduction in system dimensionality is preferable to strong dilution of the material (e.g., with inert, randomly distributed nanoparticles) since the former method should maintain a sufficient percolation path for charges and excitons within the conjugated material. White electroluminescence has recently been demonstrated for devices based on these nanocomposites,<sup>15</sup> making such polymer intercalation in an inorganic matrix a promising approach towards achieving stable color-tuning of light emitters.

## ACKNOWLEDGMENTS

This work was supported by the EPSRC and the Royal Society.

\*Electronic address: p.parkinson1@physics.ox.ac.uk

†Electronic address: l.herz1@physics.ox.ac.uk

<sup>1</sup>M. Pope, H. P. Kallmann, and P. Magnante, *J. Chem. Phys.* **38**, 2042 (1963).

<sup>2</sup>L. Chen, D. W. McBranch, H.-L. Wang, R. Helgeson, F. Wudl, and D. G. Whitten, *Proc. Natl. Acad. Sci. U.S.A.* **96**, 12287

(1999).

<sup>3</sup>P. Peumans, A. Yakimov, and S. R. Forrest, *J. Appl. Phys.* **93**, 3693 (2003).

<sup>4</sup>R. Friend, R. Gymer, A. Holmes, J. Burroughes, R. Marks, C. Taliani, D. Bradley, D. Dos Santos, J. Brédas, M. Logdlund *et al.*, *Nature (London)* **397**, 121 (1999).

- <sup>5</sup>H. Sirringhaus, P. J. Brown, R. H. Friend, M. M. Nielsen, K. Bechgaard, B. M. W. Langeveld-Voss, A. J. H. Spiering, R. A. J. Janssen *et al.*, *Nature (London)* **401**, 685 (1999).
- <sup>6</sup>L. M. Herz, C. Silva, R. T. Phillips, S. Setayesh, and K. Müllen, *Chem. Phys. Lett.* **347**, 318 (2001).
- <sup>7</sup>J. Cornil, D. Beljonne, J.-P. Calbert, and J.-L. Brédas, *Adv. Mater. (Weinheim, Ger.)* **13**, 1053 (2001).
- <sup>8</sup>D. Beljonne, G. Pourtois, C. Silva, E. Hennebicq, L. M. Herz, R. H. Friend, G. D. Scholes, S. Setayesh, K. Müllen, and J. L. Bredas, *Proc. Natl. Acad. Sci. U.S.A.* **99**, 10982 (2002).
- <sup>9</sup>E. Hennebicq, G. Pourtois, G. D. Scholes, L. M. Herz, D. M. Russell, C. Silva, S. Setayesh, A. C. Grimsdale, K. Müllen, J.-L. Brédas *et al.*, *J. Am. Chem. Soc.* **127**, 4744 (2005).
- <sup>10</sup>T. Q. Nguyen, J. Wu, V. Doan, B. J. Schwartz, and S. H. Tolbert, *Science* **288**, 652 (2000).
- <sup>11</sup>T. Q. Nguyen, J. Wu, S. H. Tolbert, and B. J. Schwartz, *Adv. Mater. (Weinheim, Ger.)* **13**, 609 (2001).
- <sup>12</sup>J. Huang, G. Li, E. Wu, Q. Xu, and Y. Yang, *Adv. Mater. (Weinheim, Ger.)* **18**, 114 (2006).
- <sup>13</sup>T. W. Lee, O. O. Park, H. N. Cho, J. M. Hong, C. Y. Kim, and Y. C. Kim, *Synth. Met.* **122**, 437 (2001).
- <sup>14</sup>N. Ananthakrishnan, G. Padmanaban, S. Ramakrishnan, and J. R. Reynolds, *Macromolecules* **38**, 7660 (2005).
- <sup>15</sup>E. Aharon, M. Kalina, and G. L. Frey, *J. Am. Chem. Soc.* **128**, 15968 (2006).
- <sup>16</sup>E. Aharon, A. Albo, M. Kalina, and G. L. Frey, *Adv. Funct. Mater.* **16**, 980 (2006).
- <sup>17</sup>T. Förster, *Ann. Phys.* **2**, 55 (1948).
- <sup>18</sup>M. G. Kanatzidis, R. Bissessur, D. C. Degroot, J. L. Schindler, and C. R. Kannewurf, *Chem. Mater.* **5**, 595 (1993).
- <sup>19</sup>M. H. Chang, M. J. Frampton, H. L. Anderson, and L. M. Herz, *Appl. Phys. Lett.* **89**, 232110 (2006).
- <sup>20</sup>G. D. Scholes, *Annu. Rev. Phys. Chem.* **54**, 57 (2003).
- <sup>21</sup>P. Anfinrud, R. L. Crackel, and W. S. Struve, *J. Phys. Chem.* **88**, 5873 (1984).
- <sup>22</sup>P. K. Wolber and B. S. Hudson, *Biophys. J.* **28**, 197 (1979).
- <sup>23</sup>J. Baumann and M. D. Fayer, *J. Chem. Phys.* **85**, 4087 (1986).
- <sup>24</sup>A. Dogariu, R. Gupta, A. J. Heeger, and H. Wang, *Synth. Met.* **100**, 95 (1999).
- <sup>25</sup>L. M. Herz, C. Silva, A. C. Grimsdale, K. Müllen, and R. T. Phillips, *Phys. Rev. B* **70**, 165207 (2004).
- <sup>26</sup>S. Karabunarliev, M. Baumgarten, E. R. Bittner, and K. Müllen, *J. Chem. Phys.* **113**, 11372 (2000).
- <sup>27</sup>S. Karabunarliev, E. R. Bittner, and M. Baumgarten, *J. Chem. Phys.* **114**, 5863 (2001).
- <sup>28</sup>A. Blumen and J. Manz, *J. Chem. Phys.* **71**, 4694 (1979).
- <sup>29</sup>K. F. Riley, M. P. Hobson, and S. J. Bence, *Mathematical Methods for Physics and Engineering* (Cambridge University Press, Cambridge, England, 2000).
- <sup>30</sup>G. Duportail, F. Merola, and P. Lianos, *J. Photochem. Photobiol., A* **89**, 135 (1995).
- <sup>31</sup>Mette M.-L. Grage, Y. Zaushitsyn, A. Yartsev, M. Chachisvilis, V. Sundström, and T. Pullerits, *Phys. Rev. B* **67**, 205207 (2003).
- <sup>32</sup>J. Cornil, D. A. dos Santos, X. Crispin, R. Silbey, and J. L. Brédas, *J. Am. Chem. Soc.* **120**, 1289 (1998).